VOLUME 3, NUMBER 4, APRIL 2003

NANO LETTERS

Using Nanografting to Achieve Directed Assembly of de novo Designed Metalloproteins on Gold

Martin A. Case,*,† George L. McLendon,†,‡ Ying Hu,†,‡ T. Kyle Vanderlick,‡ and Giacinto Scoles†,‡

The Department of Chemistry and Princeton Materials Institute, Princeton University, Princeton, New Jersey 08544

Received September 16, 2002; Revised Manuscript Received September 30, 2002

ABSTRACT

Parallel three-helix bundle metalloproteins incorporating C-terminal thiol groups have been designed to orient vertically on a gold(111) surface. A small area of pre-assembled octadecanethiol was exchanged with the proteins under the action of an AFM tip. The resulting "nanografted" metalloprotein was imaged at low applied force. The measured height of the octadecanethiol monolayer was 2.2(1) nm and the mean height above this of the grafted metalloprotein layer was 3.1(4) nm. Thus the total height of the grafted metalloprotein is 5.3(4) nm. The predicted height of the vertically oriented metalloprotein is 5.2 nm. We take this as good evidence for spatial control of monolayer assembly of three-helix bundles with predictable orientation.

Natural proteins can exhibit exquisite molecular recognition of small molecules (mw < 1000). Such selective binding is a prerequisite for the design of sensor devices of all kinds, and biosensors in particular. The key to this selectivity lies in the enormous combinatorial repertoire of "host" sites that can be constructed from the twenty naturally occurring amino acids. One approach to biosensor design has been to harness biological macromolecules, coupling molecular recognition to an appropriate detection device. Such a device may be an electronically addressable substrate upon which the responsive element may be mounted.[1] Very useful in this context is the technique of atomic force microscopy (AFM), which allows the visualization, at unprecedented resolution, of surfaces in mixed solid−aqueous phases.[2−4] This has allowed researchers not only to arrange biologically relevant molecules on a variety of surfaces but also to confirm their positioning and integrity.[5,6] Such molecular level confidence in a system is invaluable for the design and realization of biomolecular devices capable of predictable function.

The fabrication of biosensors has traditionally been centered on the choice of a natural biomolecule that exhibits the desired physicochemical properties in solution. Minimal modification is then undertaken in order to anchor the system in an appropriate matrix while preserving as best as possible the necessary function. This strategy has been successfully implemented in the work of Boussaad et al.,[7,8] although such approaches tend to be limited by the often fragile physical

* Corresponding author. Telephone 609-258-1371; Fax 609-258-6746; E-mail: macase@princeton.edu
† The Department of Chemistry, Princeton University.
‡ Princeton Materials Institute, Princeton University.

10.1021/nl025795h CCC: $25.00
Published on Web 10/26/2002

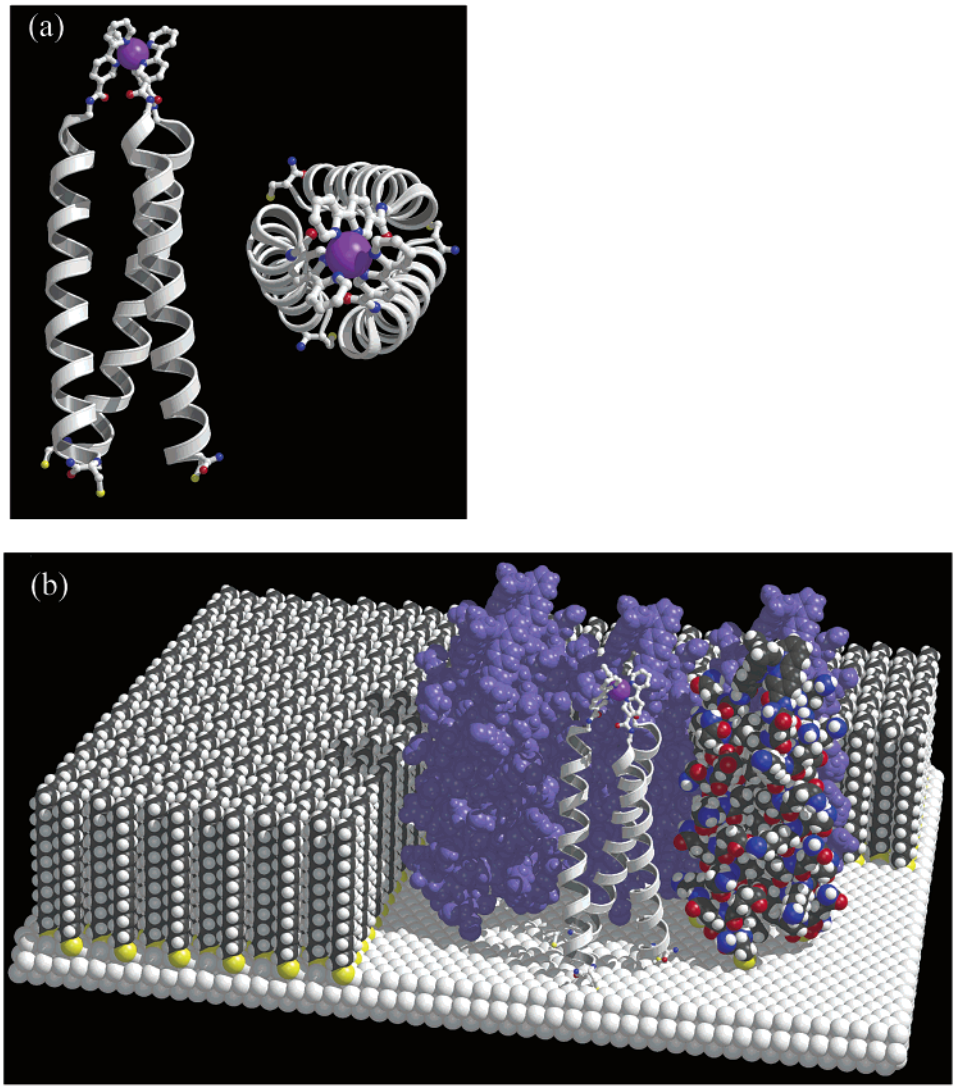

Figure 1. Schematic illustrations of three-helix bundle metalloproteins $[Fe(\alpha pV_aL_dC26)_3]^{2+}$. (a) Ribbon diagrams showing the coiled-coil fold, top and side views. The $[Fe(bpy)_3]^{2+}$ and D-cysteine residues are shown in ball-and-stick representation. (b) Model of six three-helix metalloproteins grafted into a C_{18} SAM. One of the proteins is shown as in (a), one is in color-coded space-filling representation, and the remainder are shown as van der Waals surfaces. The C_{18} monolayer is shown without the 30° tilt for clarity.

characteristics of the immobilized biomolecule. Such systems may be further destabilized by the anchoring chemistry or by the proximity of the substrate.

We have attempted to circumvent some of these problems by designing structurally robust proteins adapted for predictable adsorption to surfaces. To probe the successful surface assembly of these proteins, we have adopted the strategy of nanografting,[9] by which submicron-scale areas of a self-assembled monolayer on a gold substrate may be patterned by tip-induced chemical exchange with a different molecule. Nanografting offers several clear advantages for this type of work: (1) it allows investigation of a conveniently small region with well-defined boundaries; (2) the technique is inherently nanoscale and lends itself to the patterning of multifunctional devices by the sequential adsorption of a series of proteins with different functionality in different addressable locations; (3) it allows the measurement of molecular heights above the substrate with sufficient precision (<10%) to identify molecular orientation for all but the most spherical molecules; and (4) last but not least nanografting provides a thiol-rich substrate in which even sterically hindered thiol functionalities may find a pathway, by exchange with the smaller alkanethiols, to bind to the surface rapidly.

The past 10 years have seen an enormous increase in the understanding of protein folding and application of this understanding to de novo protein design. It is no longer unusual to see reports of designed proteins in the literature, and the principles of design of motifs such as coiled coils are well established.[10−17] We have chosen to work with a subset of this general fold, the parallel three-stranded coiled coil. Such systems can be selectively assembled by appropriate choice of hydrophobic core residues. For example, a repeat of the hydrophobic amino acids leucine (L) and valine (V) at the first and fourth positions of a heptad of amino acids has been reported to confer trimeric specificity over dimeric, tetrameric, etc. aggregation states.[18] For shorter peptides (less than 30 amino acids), however, such specificity may not be as marked. For this reason we use a design that exploits the coordination requirements of transition metal ions

in order to dictate the topology of the resulting multipeptide ensemble.[19−23]

Specifically, each peptide has a bidentate 2,2′-5-carboxybipyridyl ligand appended covalently via an amide linkage to the N terminus. Addition of ferrous iron sequesters three such ligands to form the octahedral $[Fe(bpy)_3]^{2+}$ complex. Formation of the complex increases the effective local peptide concentration, and the ensuing hydrophobic collapse of the interior of the structure is accompanied by folding of the tertiary parallel three-helix bundle protein architecture. The folded structure is designed to present the C-termini of the three helices to an appropriate surface in a tripodal manner. To facilitate assembly on gold, the helices were terminated with D-cysteine residues. The β-thiols enable the necessary chemisorption to gold and the unnatural D-stereochemistry presents them coaxially with the helices rather than equatorially, which would be the case were L-cysteine to be employed. We here report the results of nanografting the 78 amino acid iron(II) complex $[Fe(\alpha pV_aL_dC26)_3]^{2+}$ (Figure 1) into a C_{18} alkanethiol monolayer previously assembled on a Au(111) surface. Experiments were also attempted using the truncated 19-residue analogue $[Fe(\alpha pV_aL_dC19)_3]^{2+}$.

The process of nanografting has been described extensively elsewhere.[9] Briefly, a monolayer of (for example) a C_{18} alkanethiol is allowed to self-assemble on a gold surface by exploiting the affinity of thiols for elemental gold. An AFM tip can then be used at a low applied force (typically <10 nN) to image the surface morphology (sometimes achieving molecular resolution) to select a flat region. If the force is then increased (the precise increase is determined by the tip radius) in the presence of a solution containing a different molecule, the AFM tip can stimulate exchange between the new molecules and those comprising the monolayer throughout the region of interest. The alkanethiols displaced from the SAM are subject to extremely high dilution in the liquid cell and have little opportunity to return to the gold surface. Subsequent imaging of the selected area, again at low force, allows visualization of the exchanged molecules. If the height of the SAM is known, one can image the exchanged molecules by virtue of a height difference. Such height difference between the SAM and the grafted molecule is, however, not a prerequisite for successful imaging, as the new patch inevitably exhibits different properties (particularly friction) than the bulk SAM.

To test the reliability of measured height differences, a patch of C_{10} alkanethiol was grafted into the C_{18} SAM. The results are shown in Figure 2. The measured height difference was 0.90(4) nm. The calculated height difference, assuming a hydrocarbon chain tilt angle of 30°, is 0.86 nm. The grafting experiments were conducted over a range of applied force. Below a force of 15 nN, incomplete patterns are formed. At applied forces above this threshold, complete patterns are formed with one pass. At still higher applied forces, the tip and the gold substrate are irreversibly damaged.

While such experiments are conveniently performed in 2-butanol (see Supporting Information), it is unlikely that protein structure can be maintained in such milieu. Conversely, the aqueous environment necessary to induce the tertiary protein structure is not expected to be optimal for the necessary solvation and transport of the alkanethiols displaced during the grafting process. It was found that these problems could be overcome by the addition of trifluoroethanol (TFE, 10% v/v) to the aqueous buffer. Not only does this allow for the solubilization of alkanethiols, it is also expected to induce helicity in the protein with a concomitant increase in stability. Solution stability data for $[Fe(\alpha pV_aL_dC26)_3]^{2+}$ (with and without TFE) and $[Fe(\alpha pV_aL_dC19)_3]^{2+}$ (with TFE) are presented in Figure 3. It is apparent that the addition of 10% TFE dramatically increases the stability of the protein. At 6 M guanidinium hydrochloride $[Fe(\alpha pV_aL_dC26)_3]^{2+}$ is only one-third unfolded, whereas in the absence of TFE the protein is 90% unfolded. The high stability of $[Fe(\alpha pV_aL_dC26)_3]^{2+}$ in 10% TFE precludes acquisition of a complete unfolding data set, and the free energy of folding cannot be reliably determined from the plot.

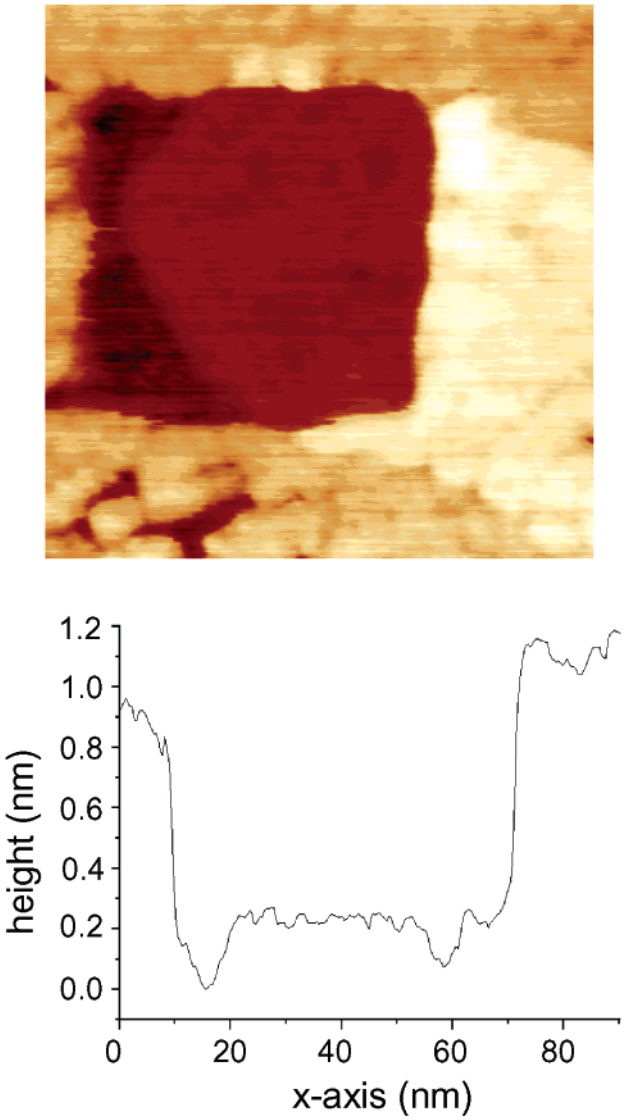

Figure 2. C_{10} grafted into a C_{18} SAM (100 nm × 100 nm) and the measured height differences: Δh(calc) = 0.86 nm, Δh(obs) = 0.90(4) nm. Steps in the gold surface are clearly visible in both figures.

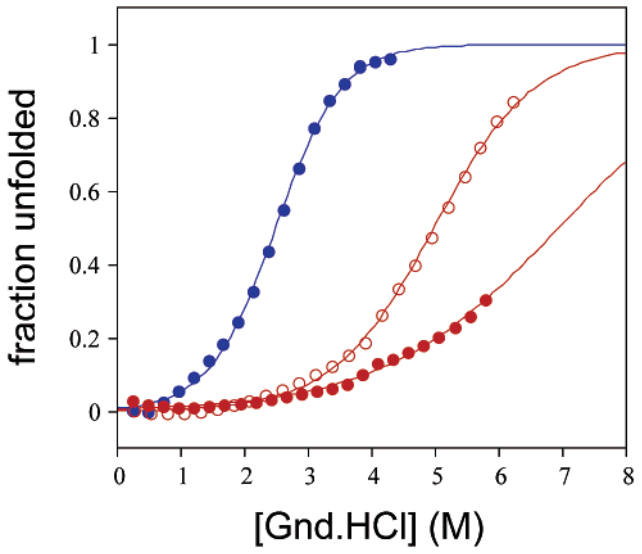

Figure 3. Chemical denaturation of $[Fe(\alpha pV_aL_dC26)_3]^{2+}$ (solid red circles) and $[Fe(\alpha pV_aL_dC19)_3]^{2+}$ (solid blue circles) in the presence of 10% TFE, and $[Fe(\alpha pV_aL_dC26)_3]^{2+}$ without TFE (empty red circles). Calculated free energies of folding are: $[Fe(\alpha pV_aL_dC19)_3]^{2+}$ 2.8 kcal M^{-1}; $[Fe(\alpha pV_aL_dC26)_3]^{2+}$ (without TFE) 3.7 kcal M^{-1}; $[Fe(\alpha pV_aL_dC26)_3]^{2+}$ (with TFE) could not be reliably determined.

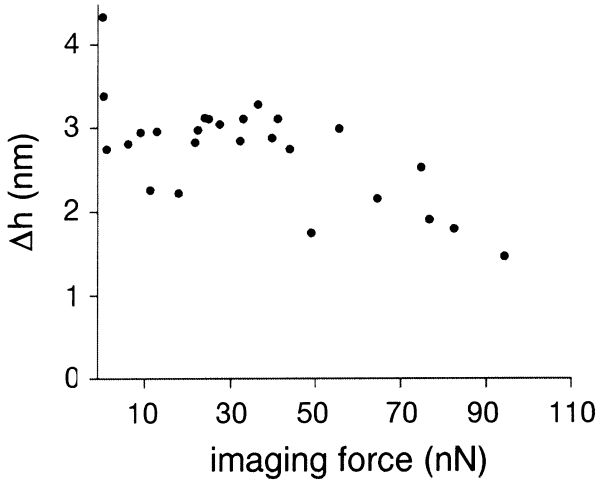

Figure 4. Height differences (protein to C_{18} SAM) vs imaging force.

Grafted protein patterns were imaged at different applied forces (Figure 4). It is clear that forces larger than 40 nN disrupt the adsorbed proteins as evidenced by an apparent decrease in measured height. Imaging was thus conducted at forces in the range 1 nN to 15 nN. The histogram of measured height differences between the grafted protein and the C_{18} SAM is shown in Figure 5a. The average value of the height difference is 3.1(4) nm, giving a measured height for the proteins of 5.3(4) nm. This compares well with the height of 5.2 nm predicted from molecular models. It is also noteworthy that the relatively large size of the protein (and hence its low diffusion coefficient in solution) slows the nanografting process significantly (as compared to the grafting of a C_{10} alkanethiol). To form compact layers, the AFM tip must be drawn slowly over the area to be grafted. If the motion of the tip is too rapid, "holes" appear in the

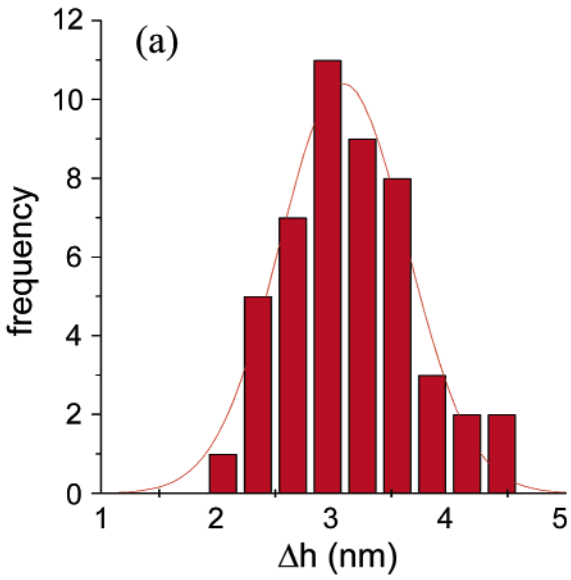

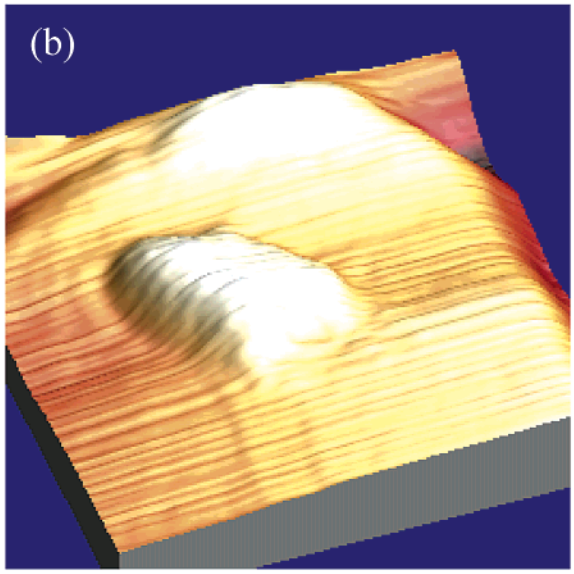

Figure 5. (a) Histogram of 48 measurements for 7 protein patches of the kind shown in (b) of the height-differences Δh between the patch surface and the surface of the SAM matrix. The forces used in the height measurements were at all times smaller than 15 nN. The continuous line on the left corresponds to a Gaussian fit centered on the value 3.1(4) nm. The patch is distorted (from a square to a parallelogram) due to thermal drift at the slow scan speed used in the grafting.

SAM which slowly fill with protein molecules. In such cases the quality of the grafted regions is inferior to those obtained when the tip moves slowly. A typical grafted protein patch is shown in Figure 5b.

Spontaneous exchange of proteins with the C_{18} SAM was also investigated. A solution of $[Fe(\alpha pV_aL_dC26)_3]^{2+}$ was allowed to exchange with a freshly prepared C_{18} SAM for 12 h. The results of subsequent AFM imaging are shown in Figure 6. Small patches of adsorbed metalloprotein (5−25 molecules) are observed with a measured height of 2.2(2) nm above the C_{18} SAM.

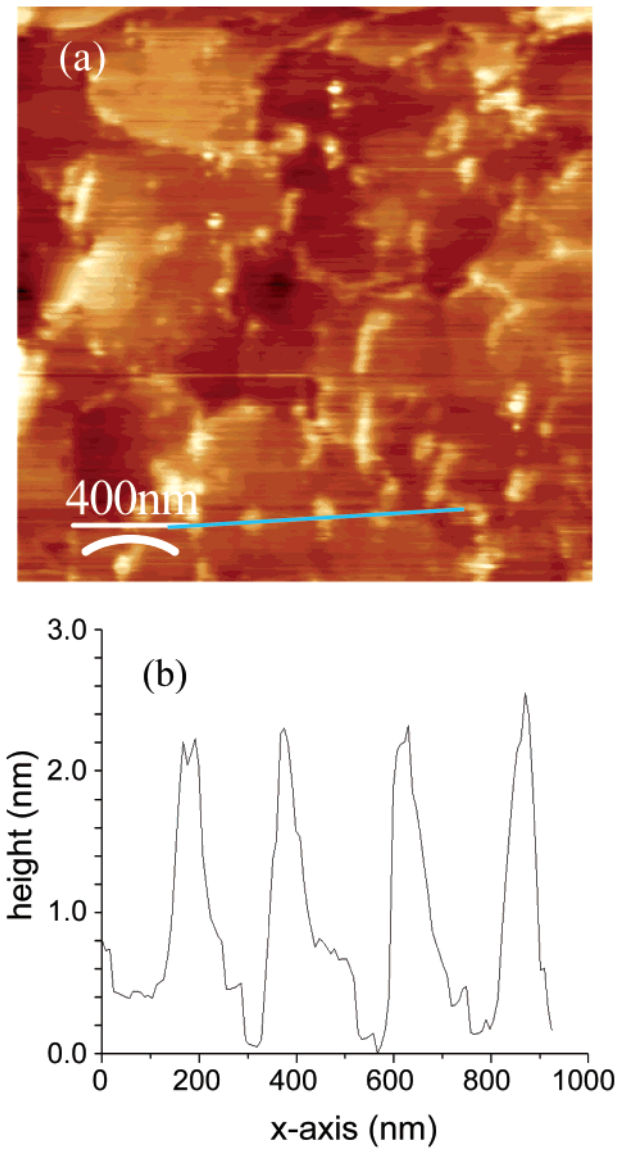

Figure 6. (a) AFM features produced by $[Fe(\alpha pV_aL_dC26)_3]^{2+}$ metalloproteins after exchange reactions with a C_{18} SAM on Au-(111). (b) Typical height measurements for the series of features crossed by the blue line at the bottom of (a).

Interestingly, monolayers of the shorter complex $[Fe(\alpha pV_aL_dC19)_3]^{2+}$ could not be grafted into the C_{18} SAM with the same clear height distribution. In these experiments, a broad distribution of low heights (0.8(5) nm) was observed. It is likely that the hydrophobic gold surface is capable of unfolding the three-helix bundle on contact, and the additional 900 cal M^{-1} stability conferred by the additional two turns per helix in $[Fe(\alpha pV_aL_dC26)_3]^{2+}$ is necessary to overcome this.[24]

In conclusion, the metal-assembled three-helix bundle $[Fe(\alpha pV_aL_dC26)_3]^{2+}$ adopts a vertical orientation, normal to a gold(111) substrate onto which it has been grafted. The measured height of the protein is 5.3(4) nm, in good agreement with molecular models. This study opens the way for a second generation design in which molecular recognition elements can be built into the surface-bound three-helix architecture.[25]

Acknowledgment. G.S., Y.H., and T.K.V. thank Professor Gang-yu Liu for her help in acquiring the nanografting know-how that has made this work possible. The work was supported in part by the National Science Foundation, award CHE0106342 (M.A.C. and G.L.M.), in part by the DOE, grant DE-FG02-93ER45503 (G.S. and G.L.M.), and in part by the NSF funded Princeton MRSEC group grant, (T.K.V.).

Supporting Information Available: Experimental details. This material is available free of charge via the Internet at http://pubs.acs.org.

References

(1) Collings, A. F.; Caruso, F. *Rep. Prog. Phys.* **1997**, *60*, 1397−1445.
(2) Amro, N. A.; Kotra, L. P.; Wadu-Mesthrige, K.; Bulychev, A.; Mobashery, S.; Liu, G. Y. *Langmuir* **2000**, *16*, 2789−2796.
(3) Fotiadis, D.; Scherring, S.; Muller, S. A.; Engel, A.; Muller, D. J. *Micron* **2002**, *33*, 385−397.
(4) Muller, D. J.; Engel, A. *Methods Cell Biol.* **2002**, *68*, 257−299.
(5) Liu, G. Y.; Amro, N. A. *Proc. Natl. Acad. Sci., U.S.A.* **2002**, *99*, 5165−5170.
(6) O'Brien, J. C.; Stickney, J. T.; Porter, M. D. *Langmuir* **2000**, *16*, 9559−9567.
(7) Boussaad, S.; Tao, N. J. *J. Am. Chem. Soc.* **1999**, *121*, 4510−4515.
(8) Boussaad, S.; Dziri, L.; Arechabaleta, R.; Tao, N. J.; Leblanc, R. M. *Langmuir* **1998**, *14*, 6215−6219.
(9) Liu, G. Y.; Xu, S.; Qian, Y. *Acc. Chem. Res.* **2000**, *33*, 457−466.
(10) Woolfson, D. N. *Curr. Opin. Struct. Biol.* **2001**, *11*, 464−471.
(11) Kohn, W. D.; Hodges, R. S. *Trends Biotechnol.* **1998**, *16*, 379−389.
(12) Micklatcher, C.; Chmielewski, J. *Curr. Opin. Chem. Biol.* **1999**, *3*, 724−729.
(13) Beasley, J. R.; Hecht, M. H. *J. Biol. Chem.* **1997**, *272*, 2031−2034.
(14) Lazar, G. A.; Hadel, T. M. *Curr. Opin. Chem. Biol.* **1998**, *2*, 675−679.
(15) Kennedy, M. L.; Gibney, B. R. *Curr. Opin. Struct. Biol.* **2001**, *11*, 485−490.
(16) Degrado, W. F.; Summa, C. M.; Pavone, V.; Nastri, F.; Lombardi, A. *Annu. Rev. Biochem.* **1999**, *68*, 779−819.
(17) Hill, R. B.; Raleigh, D. P.; Lombardi, A.; Degrado, W. F. *Acc. Chem. Res.* **2000**, *33*, 745−754.
(18) Tripet, B.; Wagschal, K.; Lavigne, P.; Mant, C. T.; Hodges, R. S. *J. Mol. Biol.* **2000**, *300*, 377−402.
(19) Gochin, M.; Khorosheva, V.; Case, M. A. *J. Am. Chem. Soc.* **2002**, *124*, 11018−11028.
(20) Lieberman, M.; Tabet, M.; Sasaki, T. *J. Am. Chem. Soc.* **1994**, *116*, 6, 5035−5044.
(21) Ghadiri, M. R.; Soares, C.; Choi, C. *J. Am. Chem. Soc.* **1992**, *114*, 825−831.
(22) Case, M. A.; Ghadiri, M. R.; Mutz, M. W.; McLendon, G. L. *Chirality* **1998**, *10*, 35−40.
(23) Case, M. A.; McLendon, G. L. *J. Am. Chem. Soc.* **2000**, *122*, 8089−8090.
(24) Contera, S. A.; Okajima, T.; Iwasaki, H. *Jpn. J. Appl. Phys. 1* **2002**, *41(6A)*, 3916−3921.
(25) Skerra, A. *J. Mol. Recognit.* **2000**, *13*, 167−187.
(26) Kraulis, P. J. *J. Appl. Crystallogr.* **1991**, *24*, 946−950.
(27) Merritt, E. A.; Bacon, D. J. *Methods Enzymol.* **1997**, *277*, 505−524.

NL025795H